

Master-Slave Synchronization of Bifurcating Integrate-and-Fire Circuits

Masanao Shimazaki, Hiroyuki Torikai and Toshimichi Saito
 Department of Electronics and Electrical Computer Engineering, HOSEI Univ.
 3-7-2, Kajino-cho, Koganei-shi, Tokyo, 184-8584, Japan.
 TEL: +81-423-87-6204, FAX: +81-423-87-6122
 E-mail : shimazaki@nonlinear.k.hosei.ac.jp

1. Abstract

We consider a master-slave pulse-coupled network of bifurcating integrate-and-fire circuits. The network exhibits in-phase chaotic synchronization and various periodic synchronization phenomena. In order to analyze these phenomena precisely, we derive a one-dimensional return map. Also using a simple test circuit, typical phenomena are demonstrated in the laboratory.

2. Introduction

In this paper we consider synchronization phenomena in a master-slave pulse-coupled network of bifurcating integrate-and-fire circuits. As a state of the master/slave reaches a firing threshold, the state is reset to a periodic base level and a pulse is generated. This is called the self-firing. The output pulse-train of the master is input to the slave. If an input pulse arrives and the slave state is above a refractory threshold, the slave fires. This is called the compulsory-firing. Due to interactions of self-firings and compulsory-firings, the network exhibits various synchronization phenomena as the following. Let the slave be periodic before the coupling. If the master is periodic, the slave exhibits compulsory-firings and self-firings and the network exhibits various periodic synchronizations. Let the slave be chaotic before the coupling. If the master is chaotic, the slave exhibits compulsory-firings and the network exhibits chaotic synchronization. If the master is periodic, the network can also exhibit various periodic synchronizations. In order to analyze these phenomena exactly, we derive a one-dimensional return map for the compulsory-firing moments. We also characterize the phenomena using a rate of compulsory-firings and self-firings. Typical phenomena are demonstrated in the laboratory using a simple test circuit.

Integrate-and-fire circuits have been studied as simplified neuron models [1][2], and their pulse-coupled neural networks (PCNNs) have been constructed. Study of synchronization phenomena of the PCNN is an important nonlinear problem, and many fundamental results have been published [3][4]. Based on periodic synchronization, applications of PCNNs have been considered, e.g., associative memory, image segmentation and combinatorial optimization problem solver [5]-[7]. However chaotic or various periodic synchronizations of PCNNs have not been considered sufficiently so far. Hence our results may contribute to develop a PCNN having some flexible function based on various synchronization phenomena. Basic results can be found in [8].

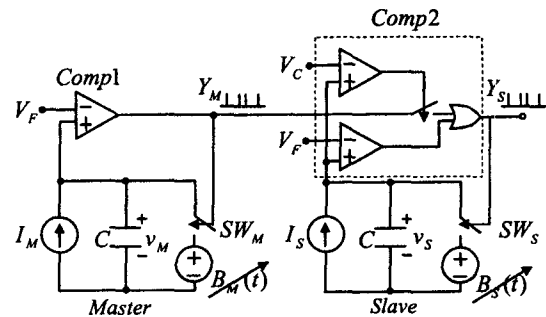


Figure 1. Master-slave pulse-coupled network.

3. Master-Slave pulse-coupled network

We consider a master-slave pulse coupled network of bifurcating integrate-and-fire circuits as shown in Fig.1. Base signals $B_M(t) = -K_M \sin(2\pi t/T)$ of the master and $B_S(t) = -K_S \sin(2\pi t/T)$ of the slave have period T and are synchronized. When the master state v_M reaches a firing threshold V_F , the master fires: a firing pulse $Y_M = V_H$ is generated, the switch SW_M is closed, and the state v_M is reset to the base $B_M(t)$. When the slave state v_S reaches a firing threshold V_F , the slave fires in a likewise master. In addition, if $V_C < v_S < V_F$ and an input pulse $Y_M = V_H$ arrives, the slave fires. Using the following dimensionless variables and parameters

$$\begin{aligned} x_M &= \frac{v_M}{V_F}, & s_M &= \frac{TI_M}{CV_F}, & k_M &= \frac{K_M}{V_F}, & \tau &= \frac{t}{T}, \\ x_S &= \frac{v_S}{V_F}, & s_S &= \frac{TI_S}{CV_F}, & k_S &= \frac{K_S}{V_F}, \\ y_M &= \frac{Y_M - V_L}{V_H - V_L}, & y_S &= \frac{Y_S - V_L}{V_H - V_L}, & th_C &= \frac{V_C}{V_F}. \end{aligned} \quad (1)$$

the network dynamics is described by

$$\begin{cases} \dot{x}_M = s_M & \text{for } x_M < 1, \\ x_M(\tau^+) = b_M(\tau^+) & \text{if } x_M(\tau) = 1, \\ y_M(\tau^+) = \begin{cases} 0 & \text{for } x_M < 1, \\ 1 & \text{if } x_M(\tau) = 1, \end{cases} \\ b_M(\tau) = -k_M \sin(2\pi\tau), \end{cases} \quad (2)$$

$$\begin{cases} \dot{x}_S = s_S & \text{for } x_S < 1, \\ x_S(\tau^+) = b_S(\tau^+) & \text{if } x_S(\tau) = 1, \\ x_S(\tau^+) = b_S(\tau^+) & \text{if } x_S(\tau) > th_C \text{ and } \\ & y_M(\tau) = 1, \\ y_S(\tau^+) = \begin{cases} 0 & \text{for } x_S < 1, \\ 1 & \text{if } x_S(\tau) = 1, \\ 1 & \text{if } x_S(\tau) > th_C \text{ and } y_M = 1, \end{cases} \\ b_S(\tau) = -k_S \sin(2\pi\tau). \end{cases} \quad (3)$$

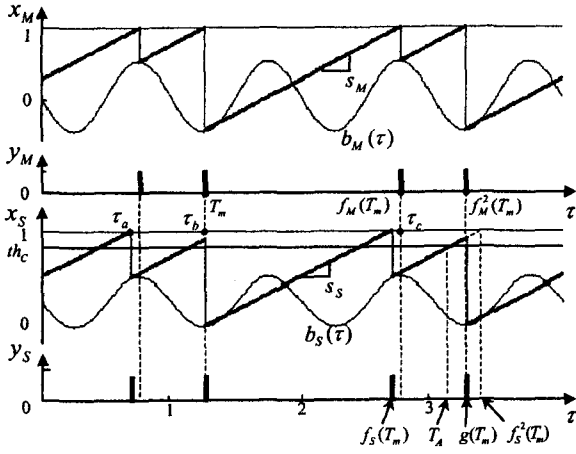


Figure 2. Basic dynamics of the network. $T_A = f_S^2(T_m) - (1 - th_C)/s_S$.

The suffixes "M" and "S" represent master and slave, respectively. k_M and k_S are the amplitudes of the bases $b_M(\tau)$ and $b_S(\tau)$. s_M and s_S are called stimulations. th_C is called refractory threshold. In this paper, we fix $s_M = 1$, $s_S = 0.95$ and $th_C = 0.8$. The controlled parameters are $|k_M| < 1$ and $|k_S| < 1$.

First, we explain the dynamics of the master (see Fig.2). If the state x_M reaches a firing threshold 1, the master outputs a firing pulse $y_M = 1$ and x_M is reset to the base $b_M(\tau)$. This is called the self-firing. Repeating the self-firings, the master generates a pulse-train $y_M(\tau)$. Letting τ_n be the n -th pulse position and letting \mathbf{R}^+ represent the positive reals, the dynamics of the pulse-train is described by a pulse position map $f_M : \mathbf{R}^+ \rightarrow \mathbf{R}^+$,

$$\tau_{n+1} = f_M(\tau_n) \equiv \tau_n - \frac{1}{s_M} b_M(\tau_n). \quad (4)$$

Noting $f_M(\tau + 1) = f_M(\tau) + 1$, we obtain a return map

$$\tau_{n+1} = F_M(\tau_n) \equiv f_M(\tau_n) \pmod{1}. \quad (5)$$

Fig.3 shows examples of the return map F_M . We note that the shape of the map f_M is determined by the shape of the base $b_M(\tau)$. Hence we can obtain various pulse-train dynamics by adjusting the shape of the base. Here we introduce the following.

Definition A pulse position τ^* is said to be periodic with period P if P is the minimum integer such that $f^Q(\tau^*) - \tau^* = P$ for some positive integer Q , where f^Q denotes the Q -fold composition of f . A pulse-train y^* is said to be periodic with period P if y^* is represented by the periodic pulse positions $(\tau^*, f(\tau^*), \dots, f^{Q-1}(\tau^*))$ and $f^Q(\tau^*) = \tau^* + P$. A periodic pulse-train y^* is said to be stable or unstable if $|Df^Q(\tau^*)| < 1$ or $|Df^Q(\tau^*)| \geq 1$, respectively, where $Df \equiv df/d\tau_n$.

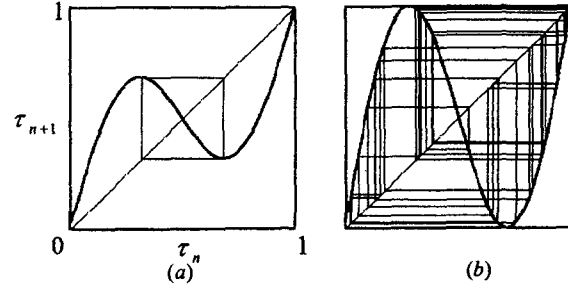


Figure 3. Return map F_M . (a) Periodic pulse-train. $k_M = 0.4$. (b) Chaotic pulse-train. $k_M = 0.73$.

Fig.3(a) corresponds to a stable periodic pulse-train, and Fig.3(b) corresponds to a chaotic (non-periodic) pulse-train.

Next, we explain the dynamics of the slave using Fig.2. If the state x_S reaches the firing threshold 1, the slave outputs a pulse $y_S = 1$, and x_S is reset to the base $b_S(\tau)$ as shown at time τ_a . This is the self-firing(SF). If $th_C < x_S < 1$ and an input pulse $y_M = 1$ arrives, the slave outputs a firing pulse $y_S = 1$ and the state x_S is reset to the base $b_S(\tau)$ as shown at time τ_b . This is called the compulsory-firing(CF). If x_S is below the refractory threshold th_C , the input pulse does not affect to the slave as shown at time τ_c . Due to the interaction of the CFs and the SFs, the network exhibits various phenomena. Note that because of the CFs, these phenomena become super-stable with respect to the initial state of the slave. Fig.4 shows typical phenomena. Letting T_m be the m -th CF moment, the dynamics of the slave is described by the following CF map:

$$T_{m+1} = g(T_m) = f_M^q(T_m), \quad (6)$$

where q is the minimum integer such that

$$f_S^p(T_m) - \frac{1}{s_S}(1 - th_C) < f_M^q(T_m) < f_S^p(T_m), \quad (7)$$

$$f_S(\tau) \equiv \tau - \frac{1}{s_S} b_S(\tau),$$

where p is some positive integer. q means the number of the SFs of the master during $T_m \leq \tau \leq T_{m+1}$. p means the number of the SFs of the slave during $T_m \leq \tau \leq T_{m+1}$. We obtain the following CF return map:

$$T_{m+1} = G(T_m) \equiv g(T_m) \pmod{1}. \quad (8)$$

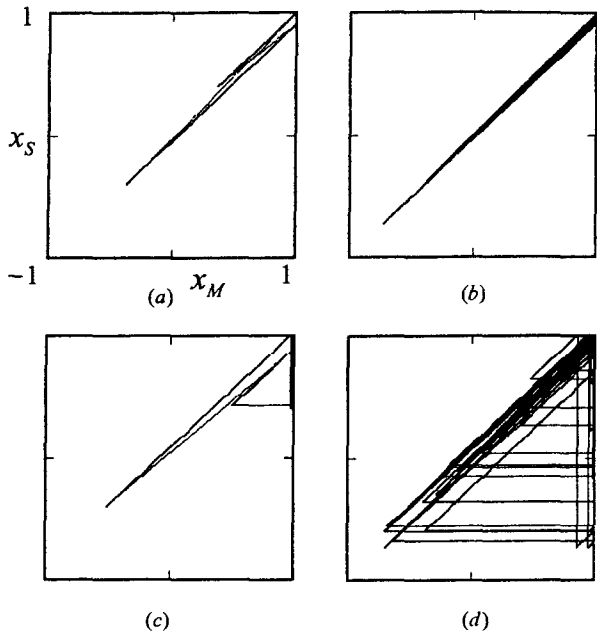


Figure 4. Phase space trajectories. (a)&(c): Periodic slave. $k_S = 0.4$. (b)&(d): Chaotic slave. $k_S = 0.73$. (a) $k_M = 0.4$ and $R_C = 1$. (b) $k_M = 0.73$ and $R_C = 1$. (c) $k_M = 0.5$ and $R_C = 0.5$. (d) $k_M = 0.7$ and $R_C \simeq 0.67$.

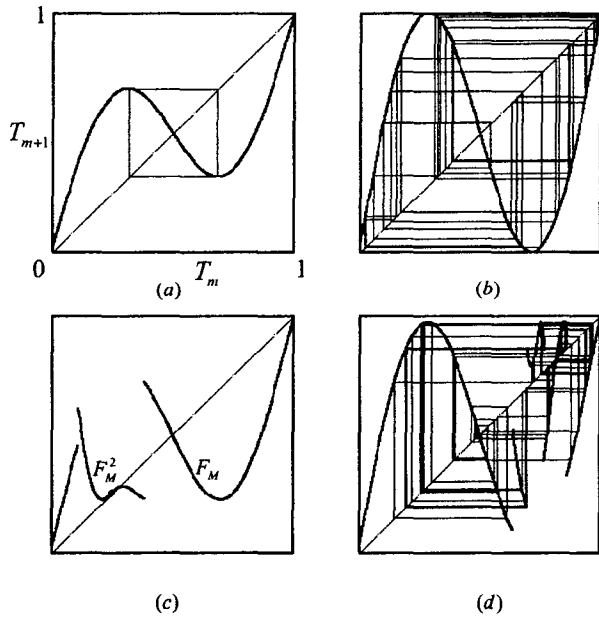


Figure 5. CF return map. (a)&(c): Periodic slave. $k_S = 0.4$. (b)&(d): Chaotic slave. $k_S = 0.73$. (a) $k_M = 0.4$ and $R_C = 1$. (b) $k_M = 0.73$ and $R_C = 1$. (c) $k_M = 0.5$ and $R_C = 0.5$. (d) $k_M = 0.7$ and $R_C \simeq 0.67$. (a)-(d) correspond to Fig.4(a)-(d).

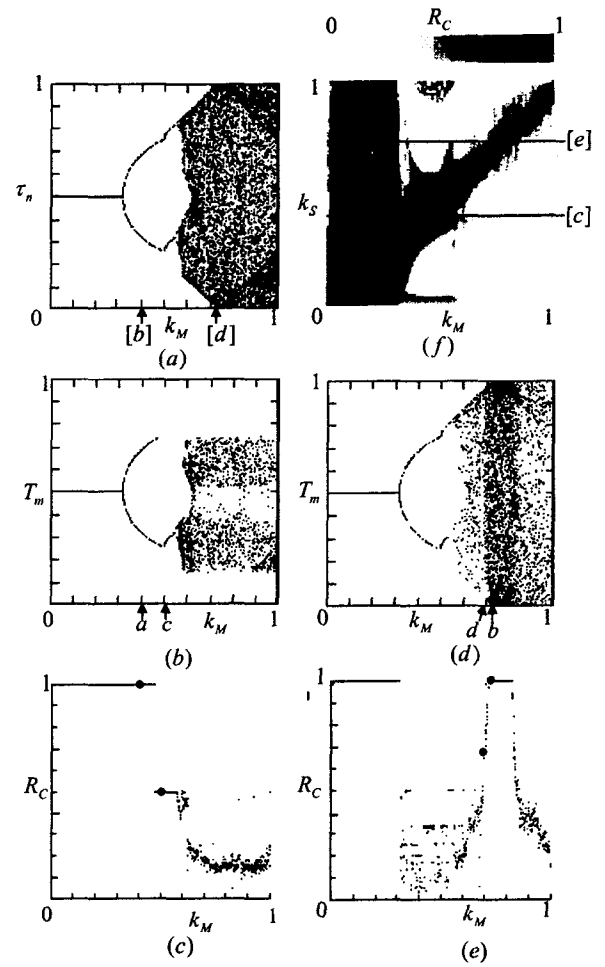


Figure 6. (a) Bifurcation diagram of SF moment τ_n of the master. (b)&(d) Bifurcation diagram of CF moment T_m of the slave. (b) $k_S = 0.4$. (d) $k_S = 0.73$. (c),(e)&(f) CF rate R_C . (c) $k_S = 0.4$. (e) $k_S = 0.73$. [b]-[e] correspond to (b)-(e). a-d correspond to Fig.4(a)-(d).

Fig.5 shows CF return map. In order to characterize these phenomena, we introduce a CF rate R_C as the following:

$$R_C \equiv \frac{N_C}{N_S + N_C}, \quad (9)$$

where N_S is the number of SFs, N_C is the number of CFs, and N_C is sufficiently large. We can calculate R_C using the CF map g : the iteration number gives N_C , and the summation of p in Equ.(7) for each T_m gives $N_S + N_C$.

Fig.6(a) shows bifurcation diagram of the SF moment τ_n of the master. Let us fix the slave parameter at $k_S = 0.4$. In this case, if the slave has no pulse-train input y_M , it is periodic. Fig.6(b) and (c) show a bifurcation diagram of the CF moment T_m and the CF rate R_C for the master parameter k_M . If $R_C = 1$, the slave exhibits the CF only, and $T_m = \tau_n$. Then, the plots of the CF moment T_m are identical with the plots of the SF moment τ_n of the master. If $R_C < 1$, the slave exhibits the CFs and the SFs. Then, the plots of T_m include lighter parts and lacking parts which correspond to SFs. Next, let us fix the slave parameter at $k_S = 0.73$. In this case, if the slave has no pulse-train input y_M , it is chaotic. Fig.6(d) and (e) show a bifurcation diagram of T_m and R_C for k_M . Compared to Fig.6(b), the plots of T_m in Fig.6(d) have fewer lacking parts: a chaotic slave may synchronize with more various pulse-train input y_M than a periodic slave. Fig.6(f) shows a bifurcating diagram of R_C for k_S and k_M .

4. Implementation

We have implemented the network as the following. The base signals $B_M(t)$ and $B_S(t)$ are generated using a function generator. The circuit is implemented by NJM13600(current source), LM339(comparator), 4066(switch), 14071(OR gate) and TL071(op-amp). In order to obtain the firing pulse with appropriately short width, we added monostable multivibrators(4538) at the outputs of the comparators. Fig.7 shows laboratory measurements.

5. Conclusions

The master-slave network can exhibit various synchronization phenomena due to the interaction of the SFs and the CFs. It is suggested that a chaotic slave can synchronize with more various input pulse-trains than a periodic slave. Future problems include: 1) detailed classification and analysis of the synchronization phenomena; 2) development of the network to an artificial neural system; and 3) design of a simple implementation circuit.

References

[1] H.Torikai and T.Saito, Analysis of a quantized chaotic system, Int. J. Bifurcation and Chaos (to appear).

- [2] H.Torikai and T.Saito, Resonance phenomena of interspike intervals from a spiking oscillator with two periodic inputs, IEEE Trans. CAS-I, vol.48, no.10, 2001.
- [3] E.M.Izhikevich, Weakly Pulse-coupled oscillators, FM Interactions, Synchronization, and oscillatory associative memory, IEEE Trans. NN, vol.10, no.3, pp.508-526, 1999.
- [4] Special Issue on Spiking Neurons in Neuroscience and Technology, Neural Networks, Vol.14, No.6-7, 2001.
- [5] G. Lee and N. H. Farhat, The bifurcating neural network 2: an analog associative memory, Neural Networks, vol.15, no.1, pp.69-84, 2002.
- [6] S. R. Campbell, D. Wang & C. Jayaprakash, Synchrony and desynchrony in integrate-and-fire oscillators, Neural computation, vol.11, pp.1595-1619, 1999.
- [7] D. M. Sala & K. J. Cios, Solving graph algorithms with network of spiking neurons, IEEE Trans. Neural Networks, vol.10, no.4, pp.953-957, 1999.
- [8] H.Torikai, M.Shimazaki and T.Saito, Novel synchronization phenomena from a pulse-coupled network of chaotic integrate-and-fire neurons, Proc. INNS/IEEE IJCNN, pp.1269-1274, 2002.

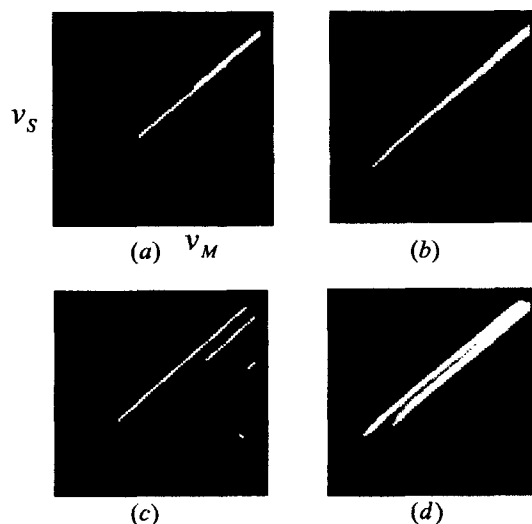


Figure 7. Laboratory measurements. $C \doteq 10$ [nF], $V_F \doteq 2$ [V], $V_C \doteq 1.6$ [V], $T \doteq 0.5$ [ms], $I_M \doteq 32$ [μ A], $I_S \doteq 29$ [μ A]. v_M and v_S : 2V/div. (a)&(b): Periodic slave. $K_S \doteq 0.8$ [V]. (c)&(d): Chaotic slave. $K_S \doteq 1.46$ [V]. (a) $k_M \doteq 0.8$ [V]. (b) $k_M \doteq 1.46$ [V]. (c) $k_M \doteq 1$ [V]. (d) $k_M \doteq 1.4$ [V]. (a)-(d) correspond to Fig.4(a)-(d).